

Received January 23, 2020, accepted February 8, 2020, date of publication February 17, 2020, date of current version February 27, 2020.

Digital Object Identifier 10.1109/ACCESS.2020.2974481

Determining the Capacity Limit of Inverter-Based Distributed Generators in High-Generation Areas Considering Transient and Frequency Stability

HEEWON SHIN ^{ORCID}, (Student Member, IEEE), JAEYEOP JUNG ^{ORCID}, (Student Member, IEEE),
AND BYONGJUN LEE ^{ORCID}, (Senior Member, IEEE)

Department of Electrical Engineering, Korea University, Seoul 02841, South Korea

Corresponding author: Byongjun Lee (leeb@korea.ac.kr)

This work was supported in part by Korea Electric Power Corporation under Grant R17XA05-4, and in part by the Human Resource Program in Energy Technology of the Korea Institute of Energy Technology Evaluation and Planning (KETEP) through the Ministry of Trade, Industry, and Energy, South Korea under Grant 20174030201820.

ABSTRACT The responses of an inverter-based distributed generator (IBDG) to abnormal voltage and frequency are different from those of a conventional generator owing to the difference in the operating modes. In particular, the momentary cessation (MC) mode deteriorates the transient stability of normal power systems by ceasing to provide active and reactive power to the grid. However, in a high-generation area, where a significant amount of generation is concentrated and where transient instability exists under a contingency, MC operation is conducive to the transient stability because the electrical output of critical generators increases to cover the local loads under this condition. This effect can cause frequency instability if a sizeable portion of the IBDG output is lost owing to the operating modes. To ensure transient and frequency stability, this study analyzed the effects of operating modes and generator tripping on the high-generation area. A method for determining the capacity limit of the IBDGs in the high-generation area was then developed to ensure power system stability. The effectiveness and feasibility of the proposed method were verified by conducting a case study on the Korean power system.

INDEX TERMS Frequency nadir, inverter-based distributed generator, momentary cessation, power system frequency stability, power system transient stability, single-machine equivalent.

I. INTRODUCTION

Renewable energy generators are increasingly preferred over coal-fired power plants owing to environmental concerns such as the rising levels of greenhouse gases and pollution. Unlike large-scale conventional generators, individual photovoltaic (PV) and wind turbine generators are generally integrated into the distribution system because they have a relatively small capacity. The power generation characteristics of inverter-based distributed generators (IBDGs) such as PV and wind turbine systems differ from those of conventional generators owing to uncertain electricity generation and use of power conversion systems. These characteristics affect the power system stability [1]–[3].

The associate editor coordinating the review of this manuscript and approving it for publication was Ning Kang ^{ORCID}.

The overall system inertia is reduced if the number of IBDGs is increased because an IBDG has very low or no rotational inertia. Various studies have been conducted to investigate the influence of IBDGs on the power system stability. The effects of distributed generators that are not connected through power electronics in a power system on the stability of transient and small signals have been analyzed [4]. This study was focused on the effects of power system stabilizers and exciters. The effects of high PV penetration on the steady-state and transient stability have been investigated [5]. The correlation between the bus voltage magnitude and PV penetration level was studied to investigate the steady-state stability. Additionally, the positive and negative influences of PV penetration on the transient stability were examined. In [6], the effects of synchronous, asynchronous, and IBDG units on the voltage and transient stability were analyzed based on a time-domain simulation. The IBDGs were found

to negatively affect the rotor angle stability. The rotor speed deviation of a conventional generator was analyzed to assess the transient stability [7]. This work considered various levels of IBDG penetration under varying contingency and demonstrated the importance of branch representation in the distribution system. The concept of a virtual synchronous generator has been proposed to improve the frequency stability in a power system with high IBDG penetration [8]. In [9], a key performance indicator was proposed to measure the frequency stability limit in a system with high penetration of power-electronic-interfaced generators. This study improved the frequency nadir (NADIR) using the fast frequency response of wind turbine generators. The effects of the penetration level of micro-grids, including IBDGs, on the frequency stability were investigated to determine the maximum allowable penetration of micro-grids in large-scale power systems [10]. In addition, the influence of variable generation of a PV system on the frequency stability was analyzed by long-term dynamic simulations [11]. However, none of these studies considered the effect of inverter operating modes on the power system stability.

The Canyon 2 Fire, Blue Cut Fire, Angeles Forest disturbance, and Palmdale Roost disturbance are some representative cases that show the negative effects of inverter operating modes on the power system stability [12]–[14]. The first two fire events caused transmission system failures in Southern California. The events resulted in the loss of a significant amount of PV generation because of the inverter operating modes, particularly the momentary cessation (MC) mode. Similarly, the Angeles Forest disturbance and Palmdale Roost disturbance led to the loss of a significant amount of PV output in Southern California in 2018. These effects were also induced by the MC of the PV systems. MC is a temporary cessation applied to energize an electric power system (EPS), while connected to the area EPS, in response to a disturbance in the applied voltage or system frequency, with the capability of immediately restoring the output when the applied voltage and system frequency return to the defined ranges [15]. According to [15], an IBDG will enter the MC mode if its terminal voltage drops below the MC voltage, which is 0.5 pu. In addition, IBDGs will trip if they remain in the MC mode for more than 1 s. The actual setting value can be different from the value specified in [15], because the value is flexible.

Recently, some studies have been performed on the effect of MC. A model of an IBDG with operating modes was introduced for reliability studies [16]–[19]. In [20], the influence of MC capability on the New England power system was investigated by a time-domain simulation. It involved composite load models with IBDGs and a system protection model. This work reported the sensitivity to voltage tripping and system response under different MC voltage levels. The effect of the MC mode of IBDGs on the power system transient stability was analyzed [21]. In addition, the MC influence index based on the critical MC operating point was proposed to evaluate the severity of transient effects. However, few studies have investigated the effect of MC on power

system stability in high-generation areas. A high-generation area represents the sending end, where a significant amount of generation is concentrated, resulting in transient instability under transmission system contingency. This area includes critical generators in terms of transient stability. Therefore, special protection schemes (SPSs), such as tripping of generators and shedding of loads, are usually implemented in the high-generation area to ensure power system stability [22]–[24].

The remainder of this paper is organized as follows: Section II investigates the effects of generator tripping and MC of IBDGs on the transient stability of the power system in the high-generation area using the single-machine equivalent (SIME) method, as described in [25]–[29]. Section III analyzes the effects of generator tripping and MC on the frequency stability of the power system by comparing the NADIRs. In Section IV, a method to determine the capacity limit of IBDGs considering both transient and frequency stability is introduced to ensure power system stability. Section V presents a case study conducted to verify the feasibility and effectiveness of the proposed method. Section VI concludes the paper.

II. EFFECTS OF GENERATOR TRIPPING AND MC OF IBDGS ON TRANSIENT STABILITY IN HIGH-GENERATION AREAS

This section analyzes the effects of generator tripping and MC of IBDGs on the transient stability of the power system based on the SIME method, which is a hybrid-direct method for transient stability assessment considering accuracy and flexibility [25]–[29]. To assess the transient stability, the generators in a system are divided into critical and non-critical groups in accordance with the SIME rules [27], [29]. In actual large-scale power systems, the critical generators are fewer than non-critical generators because only the generators located near the fault area are generally considered as critical. Furthermore, the MC capability affects a critical generator more than a non-critical generator because the IBDGs located near the critical group will enter the MC mode. Therefore, the one-machine infinite bus (OMIB) system reflecting the effect of MC is more strongly affected by the critical generators. The elements of the OMIB system in SIME are as follows.

$$\delta \triangleq \delta_C - \delta_N \quad (1)$$

$$P_m = M \left(M_C^{-1} \sum_{i \in C} P_{mi} - M_N^{-1} \sum_{j \in N} P_{mj} \right) \quad (2)$$

$$P_e = M \left(M_C^{-1} \sum_{i \in C} P_{ei} - M_N^{-1} \sum_{j \in N} P_{ej} \right) \quad (3)$$

$$M = M_C M_N / (M_C + M_N) \quad (4)$$

Here, δ is the center of angle (COA) of the OMIB system; δ_C and δ_N are the COAs of the critical and non-critical groups, respectively; P_m and P_e are the mechanical power and electrical power of the OMIB system, respectively; M is the inertia coefficient of the OMIB system; M_C and M_N are the inertia coefficients of the critical and non-critical groups, respectively; P_{mi} and P_{mj} are the mechanical power

of machines i and j , respectively; P_{ei} and P_{ej} are the electrical powers of machines i and j , respectively.

The transient stability can be assessed by comparing the maximum deceleration area A_{dec} and the acceleration area A_{acc} of the OMIB system [25]. The areas represent the release of stored and accumulated kinetic energies, respectively. If A_{acc} is greater than A_{dec} , the system will be unstable; otherwise, the system can return to a stable condition after the contingency.

A. EFFECT OF CRITICAL GENERATOR TRIPPING ON SIME

The tripping of generators realized by the SPS is usually for restoring the system stability after a contingency. The OMIB system in SIME is affected more strongly by the tripping of the critical generator than by the tripping of the non-critical generator because the number of critical generators is lower than the number of non-critical generators in a large-scale power system. When the critical generators are tripped for ensuring transient stability, the elements of the OMIB system are changed as follows:

$$P'_m = M' \left(M'^{-1}_C \sum_{k \in C} P_{mk} - M_N^{-1} \sum_{j \in N} P_{mj} \right) \quad (5)$$

$$P'_e = M' \left(M'^{-1}_C \sum_{k \in C} P_{ek} - M_N^{-1} \sum_{j \in N} P_{ej} \right) \quad (6)$$

$$M' = (M_C M_N - M_T M_N) / (M_C - M_T + M_N) \quad (7)$$

Here, P'_m and P'_e are the mechanical and electrical powers of the OMIB system after the tripping of the critical generator, respectively; k is the number of critical machines excepting the tripped generators; M' is the inertia coefficient of the OMIB system after the tripping of the critical generator; M_T is the inertia coefficient of the tripped generator.

The above equations can be used to construct the P - δ curve of the OMIB system considering critical generator tripping, as shown in Fig. 1. The generator tripping realized by the SPS operation is activated to ensure transient stability of the power system after the fault is cleared. Thus, the acceleration area is

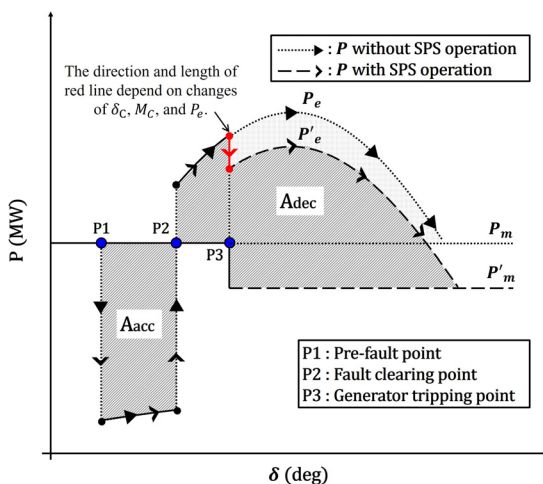


FIGURE 1. P - δ curves of OMIB system with and without SPS.

not affected by the tripped generators. However, the mechanical power of the OMIB system is reduced in the post-fault period owing to the tripped critical generators, and the maximum deceleration area increases in the transient state. The direction and length of the red line in Fig. 1 depend on how the tripped critical generators affect the OMIB system. Therefore, the deceleration area can also change because of this effect.

B. EFFECT OF MC OF IBDG ON SIME IN HIGH-GENERATION AREA

Because the MC is activated when the terminal voltage of the IBDG drops severely owing to a large disturbance, most IBDGs located near the fault area will enter the MC mode [12]–[15]. In the MC mode, the IBDGs temporarily cease to energize the power grid, and they may get tripped if they remain in the MC mode for more than 1 s [15]. The high-generation area is the generation side with large power generation; this area is susceptible to the transient stability problem under a transmission system fault. An SPS operation, such as generator tripping, is generally applied in such cases to prevent transient instability. Fig. 2 schematically illustrates the condition where the IBDGs in the high-generation area enter the MC mode or are tripped by the transmission system fault. The power transfer capability of transmission systems from a sending-end bus to a receiving-end bus decreases when the transmission line (TL) is tripped by a fault. Thereafter, the power system stability is affected by this decrease as well as by the fault.

The electrical output of a critical generator in the high-generation area is significantly affected by the MC operation and IBDG tripping, as shown in Fig. 3. If the IBDGs enter the MC mode or trip owing to severe voltage drop, the amount of

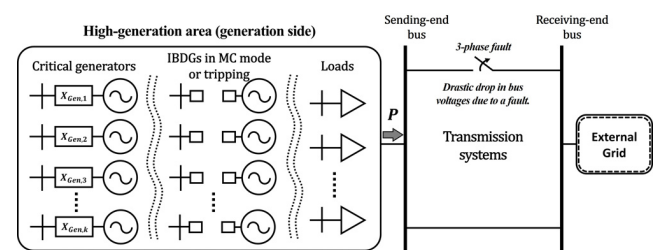


FIGURE 2. IBDG operation in the high-generation area under a contingency.

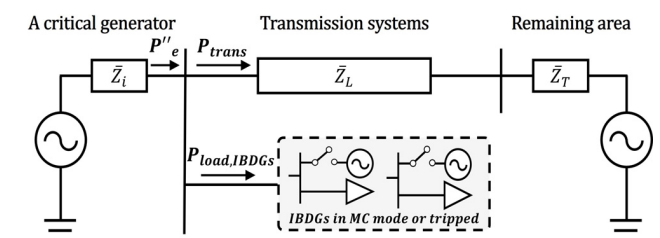


FIGURE 3. Electrical power of a critical generator in the high-generation area reflecting the MC capability.

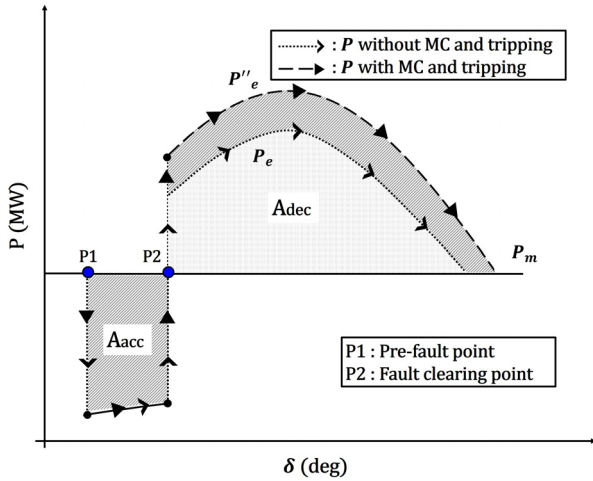


FIGURE 4. P-δ curves of a critical generator reflecting MC and IBDG tripping.

electricity generated by the IBDGs in the area is lost. The critical generators supply more electric power to cover the local loads under this condition.

Here, P''_e is the electrical output of a critical generator when the IBDGs enter the MC mode or trip; P_{trans} is the active power transferred through the transmission systems to the remaining area; $P_{load,IBDGs}$ represents the local loads considering the generation of IBDGs.

Note that $P_{load,IBDGs}$ is positive in the direction of delivery from the critical generator to the local loads with IBDGs in the high-generation area. According to (8), the electrical output of a critical generator increases as $P_{load,IBDGs}$ increases when the IBDGs enter the MC mode or trip. This implies that MC operation and IBDG tripping in the high-generation area will increase the electrical output of the critical generators, thereby improving the transient stability, as shown in Fig. 4.

$$P''_e = P_{trans} + P_{load,IBDGs} \quad (8)$$

Unlike the SPS, the effect of MC on the transient stability appears at the same time as the occurrence of a fault because the operating modes of the DG depend on the terminal voltage. More specifically, in the during-fault period, the dominant factor affecting the power system stability is the fault, and the output of the IBDG decreases to almost zero, regardless of the MC function because of the maximum converter current limit. Thus, the MC capability significantly affects the transient stability in the post-fault period.

Consequently, if the IBDGs are in the high-generation area, the deceleration area increases because of MC and IBDG tripping, leading to a positive effect of the MC function on the transient stability. The MC voltage is 0.5 pu, which is defined in [15]. In this case, the IBDGs should inject active and reactive current into the power grid unless the voltage falls below 0.5 pu due to the contingency. Because the operating mode is determined by the transient voltage level, the number of IBDGs that enter the MC mode or trip is closely related to the MC voltage. When the MC voltage increases from 0.5 to

0.9 pu, which is the continuous operating point, more IBDGs enter the MC mode even if the same fault occurs. In the high-generation area, the MC capability has a positive effect on the transient stability. Therefore, setting the MC voltage to 0.9 pu rather than 0.5 pu is advantageous for ensuring transient stability.

III. EFFECTS OF GENERATOR TRIPPING AND MC OF IBDGS ON FREQUENCY STABILITY

This section describes the negative effect of critical generator tripping and MC of IBDGs on the frequency stability of the power system.

A. EFFECT OF GENERATOR AND IBDG TRIPPING ON FREQUENCY STABILITY

The NADIR and rate of change of frequency (ROCOF) are generally used as metrics for evaluating the frequency stability [9], [30], [31]. The ROCOF of a generator and system inertia can be obtained as follows:

$$H_{sys} = \frac{\sum_{i=1}^N S_{ni}H_i}{S_{n,sys}} \quad (9)$$

$$S_{n,sys} = \sum_{i=1}^N S_{ni} \quad (10)$$

$$\frac{df_i}{dt} = \frac{f_n^2}{2 \cdot S_{ni} \cdot H_i \cdot f_i} (P_{mi} - P_{ei}) \quad (11)$$

Here, H_{sys} and $S_{n,sys}$ are the inertia constant and rated apparent power of the power system, respectively; f_i is the frequency of generator i , and f_n is the normal frequency; S_{ni} and H_i are the rated apparent power and inertia constant of generator i , respectively; P_{mi} and P_{ei} are the mechanical and electrical powers of generator i , respectively.

The ROCOF of a system can be calculated according to (9), (10), and (11), as follows [9]:

$$ROCOF(t) = \frac{\Delta P_{sys}(t)}{2(E_{kin,sys} - E_{kin,lost})} f_n \quad (12)$$

Here, $\Delta P_{sys}(t)$ is the change in the system active power; $E_{kin,sys}$ and $E_{kin,lost}$ are the kinetic energy before generator tripping and the kinetic energy lost because of generator tripping of the system, respectively.

Under severe contingency, the critical generators will be tripped by the SPS operation; the IBDGs can also trip owing to a large voltage drop. In this case, the system frequency is affected, which changes the NADIR and ROCOF, as shown in Fig. 5. To avoid load shedding, the criterion of the NADIR limit can be determined as expressed in (13). The load shedding frequency is generally defined in the grid codes.

$$f_{NADIR} > f_{UFLS} \quad (13)$$

Here, f_{NADIR} is the minimum value of the frequency in the time-domain, and f_{UFLS} is the load shedding frequency to balance the power generation and load.

Because the NADIR depends on the number of critical generators and IBDGs that are tripped following the contingency, the installed capacity of the IBDGs significantly

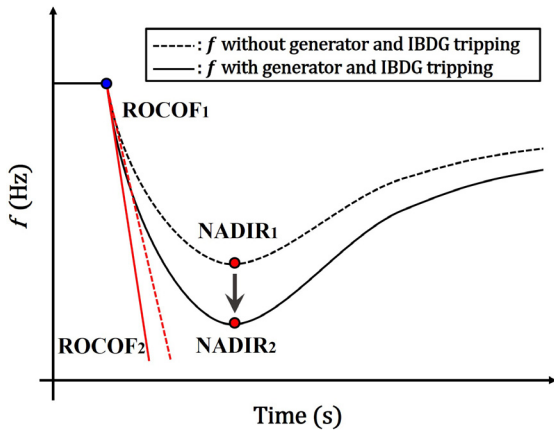


FIGURE 5. Change in NADIR and ROCOF because of generator tripping.

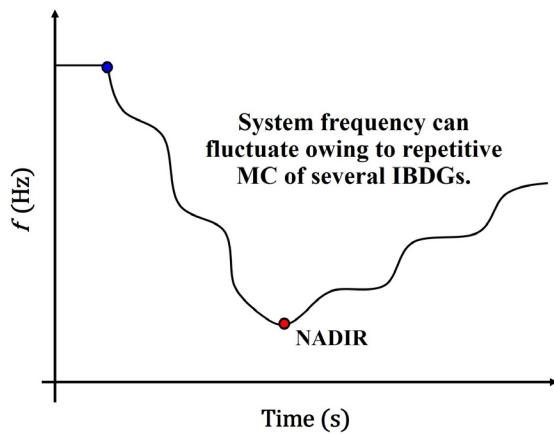


FIGURE 6. Fluctuation in the frequency due to repetitive MC operation.

affects the frequency stability. If several IBDGs are tripped due to a large disturbance, the under-frequency relay (UFR) will be operated because the NADIR decreases significantly. In addition, if the MC voltage changes from 0.5 to 0.9 pu, the frequency stability deteriorates because more IBDGs are tripped under the same contingency. Therefore, the capacity limit of the IBDGs should be determined considering the frequency stability owing to the negative effect of IBDG tripping on the frequency stability.

B. EFFECT OF REPETITIVE MC ON FREQUENCY STABILITY

Because the MC depends on the transient voltage, the IBDG can enter the MC mode repeatedly so that the active and reactive current outputs can vary continuously between zero and a maximum value. The variation in the IBDG output affects the total electrical power provided by the generators. Thus, the fluctuation in the IBDG output affects the system frequency, as shown in Fig. 6. When the MC voltage is set close to the continuous operating voltage and the IBDGs are not tripped by the MC, this effect is intensified because several IBDGs enter the MC mode repeatedly owing to the voltage disturbance.

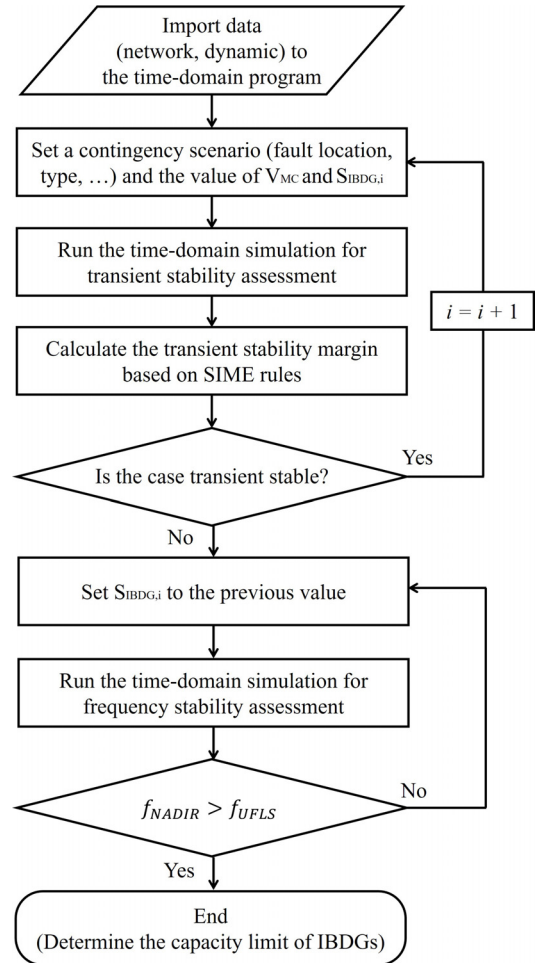


FIGURE 7. Flowchart for determining the capacity limit of IBDGs.

IV. DETERMINING THE CAPACITY LIMIT OF IBDGS CONSIDERING BOTH TRANSIENT AND FREQUENCY STABILITY

As discussed in Sections II and III, in the high-generation area, IBDGs have both positive and negative effects on the power system stability. More specifically, the IBDGs in the high-generation area positively affect the transient stability owing to MC and IBDG tripping. They negatively affect the frequency stability because IBDG tripping decreases the NADIR, and the repetitive MC affects the system frequency. Therefore, to ensure power system stability, a method to determine the IBDG capacity limit in the high-generation area is introduced in this section. Fig. 7 shows a flowchart for calculating the IBDG capacity limit. Here, S_{IBDG} is the installed capacity of the IBDGs, and V_{MC} is the MC voltage.

To accommodate as many IBDGs as possible in the high-generation area, it is preferable to set V_{MC} close to 0.9 pu instead of 0.5 pu. Because more IBDGs in the high-generation area enter the MC mode in the transient state, the transient stability is improved under the same contingency. The transient stability can be assessed in a few seconds because it is determined by the first swing, whereas assessing

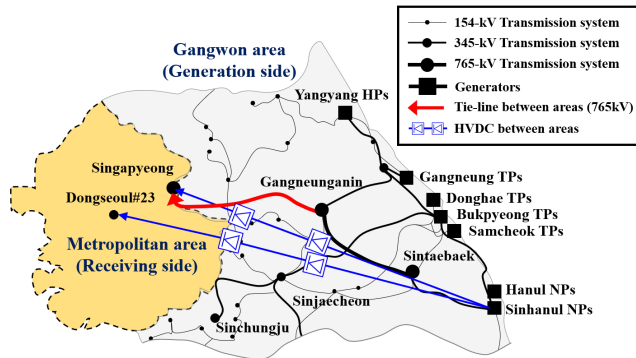


FIGURE 8. Power system configuration of the study area.

the frequency stability requires more time because of the time taken to identify the NADIR. Even S_{IBDG} , which ensures transient stability, cannot ensure frequency stability if too many IBDGs are tripped. Therefore, a frequency stability analysis must be performed after transient stability analysis to confirm the NADIR. If f_{NADIR} is lower than f_{UFLS} , the power system should not accommodate S_{IBDG} because load shedding will be initiated to prevent the power system from collapse. S_{IBDG} is determined by following the proposed method until f_{NADIR} is greater than f_{UFLS} .

V. CASE STUDY OF KOREAN POWER SYSTEM

The analysis of the effect of MC and generator tripping was performed in the Gangwon area (eastern provinces of Korea), which is the high-generation area of the Korean power system. At peak demand, the total load consumption in Gangwon is estimated to be approximately 3.9 GW in 2024. In addition, there exist thirty-seven generators, including large-scale thermal and nuclear power plants. In 2024, the total installed capacity of generators in service is expected to be approximately 21.7 GVA, and the amount of generation at peak demand is estimated to be approximately 18.1 GW. Because the generation is much greater than the load, a significant portion of the generated power is transferred from Gangwon to the Metropolitan area through high-voltage transmission systems, such as the Gangneunganin–Singapyeong TPs and high-voltage DC transmission systems. A large-scale blackout can occur if the Gangneunganin–Singapyeong TPs, which are the tie lines between Gangwon and the metropolitan, are tripped following a contingency. Therefore, the critical generators are tripped using the SPS to ensure power system stability under this contingency. The total amount of the tripped generation is approximately 2.5 GW. Fig. 8 shows the configuration of the study area.

A simulation was performed using PSS/E (Version 34.5.0). Aggregated IBDG models were connected to the distributed systems in Gangwon, which is a generation side. Economic dispatch was utilized to balance the supply and demand considering the increased IBDG capacity. In addition, the IBDGs were set to the voltage control mode and operated at unity power factor. The distributed energy

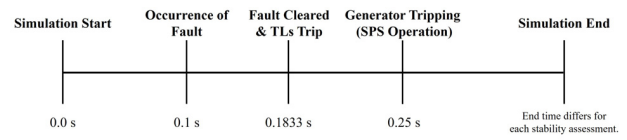


FIGURE 9. Simulation scenario in the time-domain.

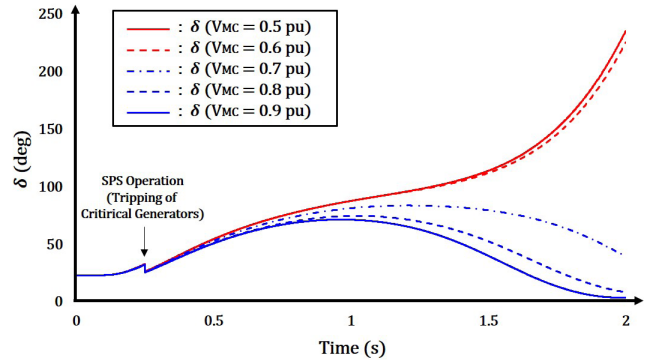


FIGURE 10. Angles of OMIB system corresponding to each MC voltage.

resource generator/converter model provided by PSS/E was used to consider the MC and tripping of the IBDG in the time-domain simulation. The parameters can be referred from [19].

The transient and frequency stabilities were evaluated under Gangneunganin–Singapyeong TPs contingency, which is a severe event in the study area. Fig. 9 shows the procedure of the time-domain simulation. A three-phase fault occurs at the sending-end bus of the Gangneunganin–Singapyeong TPs; this is normally cleared within five cycles. Thereafter, the Hanul and Sinhanul NPs are tripped through the SPS to ensure transient stability.

A. EFFECT OF IBDG IN HIGH-GENERATION AREA ON TRANSIENT STABILITY

In the time-domain simulation, the generators in Gangwon are classified as a critical group during the Gangneunganin–Singapyeong TPs contingency. Fig. 10 shows the angles of the OMIB system corresponding to each MC voltage under the contingency. In this case, the total installed capacity of the IBDGs in the high-generation area is 2.0 GVA, and the SPS is applied to ensure transient stability. When the MC voltage is set close to 0.5 pu, the transient stability deteriorates because many IBDGs remain in the high-generation area even when the critical tie lines are tripped. Therefore, in this case, if the MC voltage is set to less than 0.6 pu, the power system will become unstable even if the critical generators are tripped for transient stability.

To connect as many IBDGs as possible in the high-generation area, the MC voltage is set to 0.9 pu, and the capacity limit of the IBDGs in terms of transient stability is determined. Fig. 11 shows the angles of the OMIB system corresponding to each installed capacity of the IBDGs in the high-generation area under the contingency. Because the non-critical generators are turned off owing to the increased IBDG

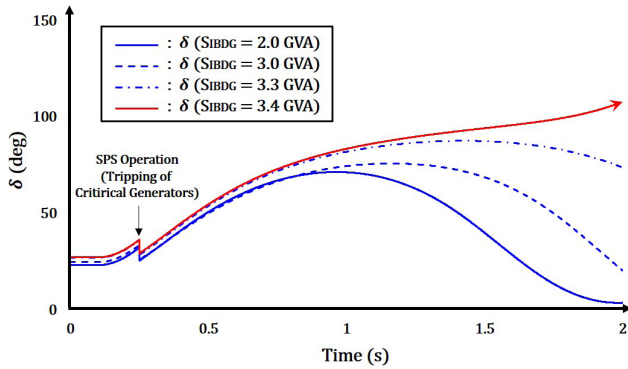


FIGURE 11. Angles of OMIB system corresponding to each installed capacity of IBDGs ($V_{MC} = 0.9$ pu).

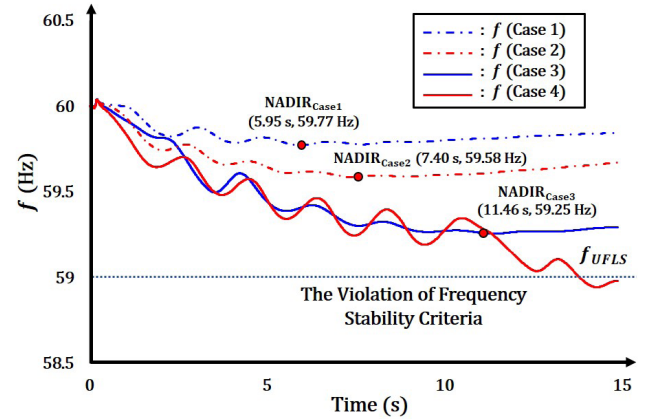


FIGURE 13. System frequencies corresponding to each case specified in Table 2.

TABLE 2. Simulation results of each scenario.

Case	IBDG capacity (MVA)	Tripped generation by SPS (GW)	Transient stability	Frequency stability
Case 1	0	2.5	Stable	Stable
Case 2	0	4	Stable	Stable
Case 3	3,300	2.5	Stable	Stable
Case 4	4,500	4	Stable	Unstable

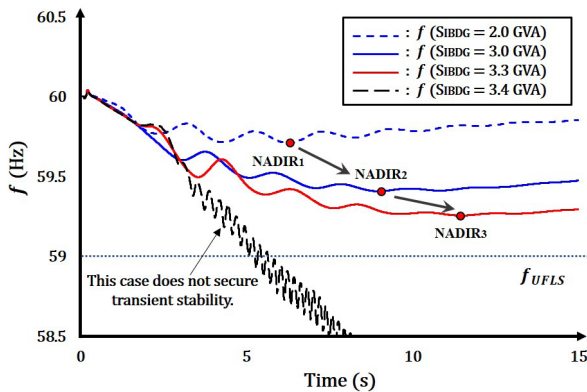


FIGURE 12. System frequencies corresponding to each installed capacity of IBDGs.

TABLE 1. Simulation results of frequencies under each IBDG capacity.

	Frequency (Hz)	Time (s)
NADIR ₁	59.710084	6.2627
NADIR ₂	59.408119	8.9739
NADIR ₃	59.255224	11.4650

capacity, the elements in the OMIB system are changed for balancing the supply and demand. Thus, the initial angles of the OMIB system differ from each other. When the installed capacity of the IBDGs increases in the high-generation area, the transient stability deteriorates because the surplus amount of electricity generated by the IBDG remains on the generation side when the power transfer capability of the transmission system is decreased because of the fault. Based on the simulation results, the capacity limit of the IBDGs in the high-generation area was determined to be 3.3 GVA through the transient stability assessment.

B. EFFECT OF GENERATOR AND IBDG TRIPPING ON FREQUENCY STABILITY

Time-domain simulations were conducted on each IBDG capacity in terms of the frequency stability to determine the capacity limit of the IBDGs in the high-generation

area by following the method established in Section IV. Fig. 12 presents the system frequencies corresponding to the installed capacity of each IBDG. Table 1 lists the simulation results for NADIRs corresponding to each IBDG capacity. Despite being subjected to the same SPS operation, the NADIR decreases as the IBDG capacity increases. This is because the amount of total generation loss is affected by the tripping of the IBDGs. If the total installed capacity of the IBDGs in the critical area is 3.3 GVA, as determined by the transient stability assessment, the NADIR should be greater than the load shedding frequency. Therefore, the capacity limit of the IBDGs in the high-generation area considering transient and frequency stability is determined to be 3.3 GVA.

C. DISCUSSION

Tripping several critical generators to increase the capacity of the IBDGs in the high-generation area may ensure transient stability but not frequency stability, as shown Fig. 13 and Table 2. In all the cases, transient stability is ensured under the contingency. However, in case 4, the frequency drops below the UFR operating point, because of which the system cannot accommodate the IBDGs. In this case, the frequency will drop continuously if a stronger SPS is not applied to the system. The ROCOFs in each case are different owing to the disposal of non-critical generators to increase the IBDG

capacity. Case 4 has the highest installed capacity of the IBDGs and large tripped generation; therefore, the ROCOF value is the highest.

VI. CONCLUSION

This study analyzed the effects of critical generator tripping and operating modes of IBDGs on the transient and frequency stability of a power system in a high-generation area. Overall, the MC capability negatively affected the transient stability, whereas the MC of the IBDGs located in the high-generation area was found to have a positive effect, similar to the case of critical generator tripping by SPS. In contrast to the positive effects on transient stability, the MC had a negative effect on the frequency stability, as indicated by NADIR and ROCOF. This is because several IBDGs and critical generators were lost due to MC operation and SPS scheme. Therefore, this study proposed a method to determine the capacity limit of the IBDGs in the high-generation area considering both the positive and negative effects.

The feasibility and effectiveness of the proposed method were validated through a case study conducted on the Korean power system. The capacity limit of the IBDGs in Gangwon, where a large number of generation sources are concentrated and where transient instability exists under TL contingency, was determined using the proposed method. Finally, we confirmed the effects of MC and generator tripping on the stability of the Korean power system.

REFERENCES

- [1] J. Guerrero, F. Blaabjerg, T. Zhelev, K. Hemmes, E. Monmasson, S. Jemei, M. Comech, R. Granadino, and J. Frau, "Distributed generation: Toward a new energy paradigm," *IEEE Ind. Electron. Mag.*, vol. 4, no. 1, pp. 52–64, Mar. 2010.
- [2] X. Xu, Z. Yan, M. Shahidehpour, H. Wang, and S. Chen, "Power system voltage stability evaluation considering renewable energy with correlated variabilities," *IEEE Trans. Power Syst.*, vol. 33, no. 3, pp. 3236–3245, May 2018.
- [3] M. A. Chowdhury, N. Hosseinzadeh, H. R. Pota, and W. Shen, "Transient stability of power system integrated with doubly fed induction generator wind farms," *IET Renew. Power Gener.*, vol. 9, no. 2, pp. 184–194, Mar. 2015.
- [4] M. K. Donnelly, J. E. Dagle, D. J. Trudnowski, and G. J. Rogers, "Impacts of the distributed utility on transmission system stability," *IEEE Trans. Power Syst.*, vol. 11, no. 2, pp. 741–746, May 1996.
- [5] S. Eftekharijad, V. Vittal, Heydt, B. Keel, and J. Loehr, "Impact of increased penetration of photovoltaic generation on power systems," *IEEE Trans. Power Syst.*, vol. 28, no. 2, pp. 893–901, May 2013.
- [6] D. Khani, A. S. Yazdankhah, and H. M. Kojabadi, "Impacts of distributed generations on power system transient and voltage stability," *Int. J. Electr. Power Energy Syst.*, vol. 43, no. 1, pp. 488–500, Dec. 2012.
- [7] E. P. Madruga, D. P. Bernardon, R. P. Vieira, and L. L. Pfischer, "Analysis of transient stability in distribution systems with distributed generation," *Int. J. Electr. Power Energy Syst.*, vol. 99, pp. 555–565, Jul. 2018.
- [8] P. F. Frack, P. E. Mercado, M. G. Molina, E. H. Watanabe, R. W. De Doncker, and H. Stagge, "Control strategy for frequency control in autonomous microgrids," *IEEE J. Emerg. Sel. Topics Power Electron.*, vol. 3, no. 4, pp. 1046–1055, Dec. 2015.
- [9] E. Rakhshani, D. Gusain, V. Sewdien, J. L. R. Torres, and M. A. M. M. Van Der Meijden, "A key performance indicator to assess the frequency stability of wind generation dominated power system," *IEEE Access*, vol. 7, pp. 130957–130969, 2019.
- [10] H. Golpira, H. Seifi, A. R. Messina, and M.-R. Haghifam, "Maximum penetration level of micro-grids in large-scale power systems: Frequency stability viewpoint," *IEEE Trans. Power Syst.*, vol. 31, no. 6, pp. 5163–5171, Nov. 2016.
- [11] K. Maslo, "Impact of photovoltaics on frequency stability of power system during solar eclipse," *IEEE Trans. Power Syst.*, vol. 31, no. 5, pp. 3648–3655, Sep. 2016.
- [12] North American Electric Reliability Corporation (NERC). (Jun. 2017). *1200 MW Fault Induced Solar Photovoltaic Resource Interruption Disturbance Report—Southern California 8/16/2016 Event*. [Online]. Available: <http://www.nerc.com/pa/rm/ea/1200MWFaultInducedSolarPhotovoltaicResourceInterruptionFinal.pdf>
- [13] *900 MW Fault Induced Solar Photovoltaic Resource Interruption Disturbance Report: Southern California 10/9/2017 Event*, North Amer. Electr. Rel. Corp., Atlanta, GA, USA, Feb. 2018.
- [14] North American Electric Reliability Corporation, "April and May 2018 fault induced solar photovoltaic resource interruption disturbances report," Tech. Rep., NERC, Atlanta, GA, USA, Jan. 2019.
- [15] *IEEE Standard for Interconnection and Interoperability of Distributed Energy Resources With Associated Electric Power Systems Interfaces*, Standard 1547-2018, IEEE Standards Coordinating Committee 21, New York, NY, USA, Feb. 2018.
- [16] B. Enayati et al., "Impact of IEEE 1547 standard on smart inverters," Nat. Grid, USA, Tech. Rep. PES-TR67, May 2018.
- [17] C. Li and R. Reinmuller, "Fault responses of inverter-based renewable generation: On fault ride-through and momentary cessation," in *Proc. IEEE Power Energy Soc. General Meeting (PESGM)*, Aug. 2018, pp. 1–5.
- [18] S. Zhu, D. Piper, D. Ramasubramanian, R. Quint, A. Isaacs, and R. Bauer, "Modeling inverter-based resources in stability studies," in *Proc. IEEE Power Energy Soc. General Meeting (PESGM)*, Aug. 2018, pp. 1–5.
- [19] D. Ramasubramanian, J. C. Boemer, P. Mitra, and A. Gaikwad, "Generic parameterization of the DER_A model," NERC Syst. Planning Impacts DER Work. Group, Austin, TX, USA, Jan. 2019.
- [20] K. Sreenivasachar, G. Zhou, and J. Senthil, "Industry experience in using the distributed energy resource (DER_A) model," Presented at the IEEE Power Energy Soc. General Meeting (PESGM), Aug. 2019.
- [21] H. Shin, J. Jung, S. Oh, K. Hur, K. Iba, and B. Lee, "Evaluating the influence of momentary cessation mode in inverter-based distributed generators on power system transient stability," *IEEE Trans. Power Syst.*, to be published, doi: 10.1109/TPWRS.2019.2942349.
- [22] P. M. Anderson and B. K. LeReverend, "Industry experience with special protection schemes," *IEEE Trans. Power Syst.*, vol. 11, no. 3, pp. 1166–1179, Aug. 1996.
- [23] D.-H. Choi, S. H. Lee, Y. C. Kang, and J.-W. Park, "Analysis on special protection scheme of Korea electric power system by fully utilizing STATCOM in a generation side," *IEEE Trans. Power Syst.*, vol. 32, no. 3, pp. 1882–1890, May 2017.
- [24] E. Ghahremani, A. Heniche-Oussedik, M. Perron, M. Racine, S. Landry, and H. Akreimi, "A detailed presentation of an innovative local and wide-area special protection scheme to avoid voltage collapse: From proof of concept to grid implementation," *IEEE Trans. Smart Grid*, vol. 10, no. 5, pp. 5196–5211, Sep. 2019.
- [25] M. Pavella and P. G. Murthy, *Transient Stability of Power Systems: Theory and Practice*. Chichester, U.K.: Wiley, 1994.
- [26] Y. Xue, T. Van Cutsem, and M. Ribbens-Pavella, "Extended equal area criterion Justifications, Generalizations, applications," *IEEE Power Eng. Rev.*, vol. 9, no. 2, pp. 38–39, Feb. 1989.
- [27] Y. Zhang, L. Wehenkel, P. Rousseaux, and M. Pavella, "SIME: A hybrid approach to fast transient stability assessment and contingency selection," *Int. J. Electr. Power Energy Syst.*, vol. 19, no. 3, pp. 195–208, Mar. 1997.
- [28] D. Ernst, D. Ruiz-Vega, M. Pavella, P. M. Hirsch, and D. Sobajic, "A unified approach to transient stability contingency filtering, ranking and assessment," *IEEE Trans. Power Syst.*, vol. 16, no. 3, pp. 435–443, Aug. 2001.
- [29] B. Lee, S.-H. Kwon, J. Lee, H.-K. Nam, J.-B. Choo, and D.-H. Jeon, "Fast contingency screening for online transient stability monitoring and assessment of the KEPCO system," *IEE Proc.-Gener., Transmiss. Distrib.*, vol. 150, no. 4, pp. 399–404, 2003.
- [30] P. Kundur, N. J. Balu, and M. G. Lauby, *Power System Stability and Control*. New York, NY, USA: McGraw-Hill, 1994.
- [31] *Future System Inertia*, ENTSO-E, Brussels, Belgium, Nov. 2013.



HEEWON SHIN (Student Member, IEEE) received the B.S. degree in electrical engineering from the Seoul National University of Science and Technology, Seoul, South Korea, in 2013. He is currently pursuing the M.S. and Ph.D. degrees with the Department of Electrical Engineering, Korea University. He will join the Korea Electrotechnology Research Institute (KERI), as a Senior Researcher. His research interests are power system analysis and operation and renewable energy integration.



BYONGJUN LEE (Senior Member, IEEE) received the B.S. degree in electrical engineering from Korea University, Seoul, South Korea, in 1987, and the M.S. and Ph.D. degrees in electrical engineering from Iowa State University, Ames, in 1991 and 1994, respectively. From 1995 to 1996, he was a Senior Researcher at Mitsubishi Electric Corporation, Kobe, Japan. Since 1996, he has been a Professor with the School of Electrical Engineering, Korea University.

...



JAEEYOP JUNG (Student Member, IEEE) received the B.S. degree in electrical engineering from Korea University, Seoul, South Korea, in 2016. He is currently pursuing the M.S. and Ph.D. degrees with the Department of Electrical Engineering, Korea University. His research interests are power system analysis and operation and renewable energy integration.